DOI: 10.1111/mice.12439

ORIGINAL ARTICLE

COMPUTER-AIDED CIVIL AND INFRASTRUCTURE ENGINEERING WILEY

Wireless charging utility maximization and intersection control delay minimization framework for electric vehicles

Zadid Khan[1] | Sakib Mahmud Khan[1] | Mashrur Chowdhury[1] | Ilya Safro[2] | Hayato Ushijima-Mwesigwa[2]

[1]Glenn Department of Civil Engineering, Clemson University, Clemson, SC, USA

[2]School of Computing, Clemson University, Clemson, SC, USA

Correspondence
Mashrur Chowdhury, Eugene Douglas Mays Professor, Glenn Department of Civil Engineering, 216 Lowry Hall, Clemson University, Clemson, SC 29634, USA.
Email: mac@clemson.edu

Funding information
National Science Foundation, Grant/Award Number: #1647361

Abstract

This study presents the Wireless Charging Utility Maximization (WCUM) framework, which aims to maximize the utility of Wireless Charging Units (WCUs) for electric vehicle (EV) charging through the optimal WCU deployment at signalized intersections. Furthermore, the framework aims to minimize the control delay at all signalized intersections of the network. The framework consists of a two-step optimization formulation, a dynamic traffic assignment model to calculate the user equilibrium, a traffic microsimulator to formulate the objective functions, and a global Mixed Integer Non-Linear Programming (MINLP) optimization solver. An optimization problem is formulated for each intersection, and another for the entire network. The performance of the WCUM framework is tested using the Sioux Falls network. We perform a comparative study of 12 global MINLP solvers with a case study. Based on solution quality and computation time, we choose the Couenne solver for this framework.

1 | INTRODUCTION

The transportation sector is characterized by the dominance of fossil fuel-powered vehicles. Due to their nonreliance on fossil fuels, electric vehicles (EVs) can help meet the environmental, economic, and energy goals if electricity is produced from environment-friendly sources such as nuclear, solar, and wind. EVs are the fastest growing alternative fuel vehicles in the market today. However, EVs have technical and economic limitations related to the electricity storage (i.e., battery) technology such as low energy density, large battery size, limited lifetime, long charging times, and high initial, operational, and maintenance cost. Beside these limitations, EV users face another difficulty known as range anxiety. EV users are constantly worrying about having enough charge in battery to complete the trips, and constantly looking for charging stations nearby when the battery is running out of charge (Egbue & Long, 2012). To overcome this, Wireless Charging Units (WCUs) on the road can transfer energy to EVs equipped with wireless charging capabilities (i.e., pick-up coils in the bottom of the vehicle) through induction, which is called dynamic charging or Charging While Driving (CWD). It can solve the issue of limited driving range by increasing the range of EVs in transit (Vilathgamuwa & Sampath, 2015). WCUs can reduce the urban space requirements for charging infrastructure of EVs. Recent developments in wireless charging technology research indicate that CWD infrastructure can be deployed for widespread use within the next 10 to 20 years (Cirimele, Freschi, & Guglielmi, 2014; Fuller, 2016; Lukic & Pantic, 2013; Vilathgamuwa & Sampath, 2015). However, a proper infrastructure planning with effective resource utilization is required to deploy this technology. Optimal placement of WCUs on the roads is a major factor in widespread adoption of CWD for EVs (Egbue & Long, 2012; Ushijima-Mwesigwa, Khan, Chowdhury, & Safro, 2017). One possible solution is to place WCUs at signalized intersections in urban areas. Vehicles stop frequently at traffic signals in urban areas and sometimes this stopped time can allow EVs to get charged. So, utilizing the stop-and-go situation at signalized intersections for wireless recharging is more appealing than charging

stations at parking lots because it saves time and increases the effective range of the EV (Mohrehkesh & Nadeem, 2011).

In this study, the focus is on framework development, which identifies the lane (or lanes) at the signalized intersections where the WCUs should be installed, and the number of WCUs that should be installed at that lane. The objective of the framework is to maximize the utility within a certain budget while minimizing the control delay of all intersections.

We define utility as the total amount of transferred energy to EVs by a WCU at a specific location within a given timeframe. The unit of utility is Watt-hour (Wh) or KiloWatt-hour (KWh). Higher utility of a certain location signifies its ability to provide more energy to EVs throughout the day, thus making it a better location to place WCUs.

The signalized intersections should operate at an acceptable Level of Service (LOS). LOS is used to express the operational condition of the traffic. There are six levels of LOS, namely level A, B, C, D, E, and F. Level A represents the best LOS with free-flow traffic operations, and level F represents the worst traffic conditions with oversaturated traffic operations (Highway Capacity Manual, 2010). For signalized intersections, LOS is used to assign traffic quality levels based on the control delay. It is the additional delay that occurs due to traffic signal compared to the case with no traffic signal. The control delay has three components: (1) uniform delay, (2) incremental delay, and (3) initial queue delay (Highway Capacity Manual, 2010). The incremental delay has two components, random delay due to occasional higher demand and deterministic delay due to sustained oversaturation conditions. The control delay is always calculated for a lane group. All the lanes in a lane group have simultaneous traffic movement, a common stop-line, and a capacity that is shared by all vehicles. In this study, control delay is estimated using the queue-count method (Highway Capacity Manual, 2010), which gives an approximate control delay per vehicle for each lane group. The input data required for this technique are collected from a traffic microsimulator. For our research, we have considered that each lane under the same lane group has similar control delay.

The basis of the problem is that a higher utility at an intersection means a higher delay. Therefore, our objective is to balance these two measures and find an optimized solution.

1.1 | Framework and its components

We present a novel framework in this article to identify the optimal placement of WCUs for a signalized roadway network in any area type and size (e.g., city, county, or state). An optimization problem is formulated and solved to find WCU placement in the network. The Wireless Charging Utility Maximization (WCUM) framework has four major components, and they are:

1. A two-step optimization problem.
2. A Dynamic Traffic Assignment (DTA) model.
3. A traffic microsimulator.
4. A global Mixed Integer Non-Linear Programming (MINLP) optimization solver.

Here, the framework uses the DTA model and the traffic microsimulator to create a calibrated simulation model. The calibrated simulation model is used to create the lane-specific utility and control delay functions. The lane-specific utility and control delay functions are fed to the first step of the optimization problem. The first step is the intersection-level optimization. We formulate a multiobjective optimization problem for each intersection; the objective functions for each intersection are total intersection utility maximization function and total intersection control delay minimization function. We use a scalarization technique to obtain one solution from the problem (Ehrgott, 2006). Scalarization can be described as formulating multiple single-objective optimization problems such that the optimal solutions to these problems form the Pareto optimal solutions to the multiobjective optimization problem. We have used the weighted-sum method (Marler & Arora, 2010) for the scalarization of our problem. The weighted-sum method offers the advantages of high search efficiency and low computational cost (Wang, Zhou, Ishibuchi, Liao, & Zhang, 2018). One of the limitations of the weighted-sum method is the requirement to bring all objectives to the same scale. We are using simulation to capture the lower and upper bounds of both objective functions, so we are able to normalize both objective functions to the same scale. By solving this problem, we obtain a Pareto-front of the solutions. However, we need only one combination of signal timing parameters, which we can use in the following step. Hence, we select only one solution from a set of Pareto optimal solutions and carry it forward. From this step, the framework identifies the traffic signal control parameters (i.e., minimum and maximum green times, gap time) for each intersection. These parameters are fed to the second step of the optimization, where a single-objective optimization problem is formulated for the whole network. There is only one objective in this step, maximization of total utility of all the lanes in the intersection. From this step, the framework identifies the lane(s) and the number of WCUs that should be installed at the selected lane(s). Section 3 describes the details of the WCUM framework development. Figure 1 shows how the framework identifies the optimal locations of WCU installation for a roadway network.

At first, the user will develop the calibrated traffic microsimulation model. The traffic microsimulation will use an energy model for calculating energy consumption and charging for each EV. The user needs to specify the EV penetration in the network and energy model parameters. The

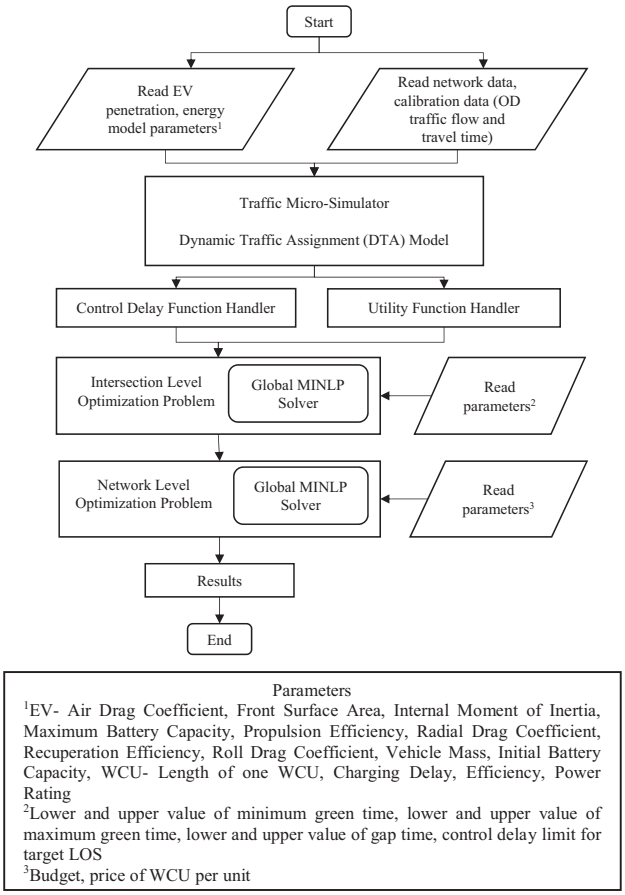

FIGURE 1 WCUM framework flowchart

calibration process is based on the Origin-Destination (OD) traffic flow and travel time data. All traffic simulation is performed after a DTA model is used to reroute the vehicles so that user equilibrium is achieved throughout the network. DTA is an iterative process that reroutes vehicles in each iteration to reduce travel times, until the travel time cannot be reduced any more. The traffic microsimulator and the routing algorithm are part of the process. After all traffic simulation is completed, the output files are fed to the utility and control delay function handlers. These two components calculate the lane-specific utility and control delays from the simulation results. These results are carried forward to the intersection-level optimization problem. The result of the intersection-level optimization is the traffic signal control parameters. These parameters are fed to the network-level optimization. For both steps, the parameters that the users need to specify are mentioned in the box below the flowchart in Figure 1. After this step, the framework outputs the solution for the network.

2 | LITERATURE REVIEW

The advancements in EV wireless charging technology have initiated substantial research on the optimal deployment of WCUs for dynamic charging applications. Many studies have been conducted on the prospects of EV wireless charging, efficient wireless charging systems, and dynamic charging scheme testing (Bi et al., 2016; Li & Mi, 2015; Qiu, Chau, Liu, & Chan, 2013). One of the significant works focuses on the system design utilizing wireless charging technology for an electric bus, also known as online EV (OLEV) (Ko & Jang, 2013). The authors have used a particle swarm optimization method to find a minimum cost solution for WCU installation. The decision variables considered in this analysis are the battery size, total number of WCUs, and places to install the WCUs on a fixed route. The model is calibrated to the actual OLEV system (Ko & Jang, 2013), which was developed by the Korea Advanced Institute of Science and Technology and deployed in Seoul, Korea (Jang, Ko, & Jeong, 2012). Other notable institutions that have successfully implemented WCU system for EVs and performed field-testing include Siemens, Volvo, Highways England, Auckland University, HaloIPT (Qualcomm), Oak Ridge National laboratory (ORNL), MIT (WiTricity), and Delphi. However, for a full commercial CWD implementation, significant changes are needed to retrofit the current transportation infrastructure.

Mohrehkesh and Nadeem (2011) have investigated wireless charging for EVs at signalized intersections. The authors propose adaptive control strategies of traffic signals for charging of EVs at intersections that would meet EV's energy demand while the control delay at intersections is minimized. This study does not focus on selecting the optimal locations for WCU installation. Earlier studies (Chen, He, & Yin, 2016; Riemann, Wang, & Busch, 2015) do not investigate the effect of traffic signals on EV charging in the analysis. One of the problems with mathematical models, which are not validated with reliable traffic simulation software, is that they often do not accurately capture the realistic traffic scenarios. In addition, most of the existing optimization models are computationally expensive as they typically contain nonlinear and nonconvex components with integer variables. As a result, they are more applicable for small networks. Ushijima-Mwesigwa et al. (2017) have introduced an integer-programming model that is built upon considering different realistic scenarios of routes. The authors have compared the computational results for the proposed model with faster heuristics and demonstrated that their approach provides significantly better results for fixed budget models. Using standard optimization solvers with parallelization, they have succeeded to provide fast and high-quality solutions for much larger networks. However, they do not consider microscopic traffic flow modeling in an urban area. Factors such as vehicular interaction and delay due to traffic signals are not considered. The Sioux Falls network, which has been used in this study, has been previously used in other studies for developing network equilibrium models for battery EVs (He, Yin, & Lawphongpanich, 2014) and

optimization models for deployment of public EV charging stations (Li, Huang, & Mason, 2016).

Recent studies focus on energy optimization of EVs (Bhavsar, He, Chowdhury, Fries, & Shealy, 2014; He, Chowdhury, Pisu, & Ma, 2012) and ITS technologies to facilitate smart charging of EVs (Johnson, Chowdhury, He, & Taiber, 2012, 2013; Sarkar et al., 2016). Deflorio, Guglielmi, Pinna, Castello, and Marfull (2015) develop a design framework for EV charging infrastructure based on the WCU performance. In another analysis, Gill et al. (2014) focus specifically on the costs of developing a wireless charging infrastructure. After analyzing the costs, the authors propose a business model which will make the implementation of the wireless charging infrastructure a profitable investment. The studies show that a typical standalone EV wireless charger with Level 2 power ratings for one EV can cost around US$1,000–US$2,000. Considering other infrastructural costs, equipping a road segment with wireless charging may cost as much as US$250K–US$500K. Therefore, the cost is a major obstacle for large-scale deployment of WCU for EVs. In general, cost of installing electric infrastructure is very high. In one study, the authors have discussed the cost of electric infrastructure for the railway system (Caíno-Lores, García, García-Carballeira, & Carretero, 2017).

Optimization of signal timing parameters using traffic microsimulation is a popular research topic. In one study, the authors have created an optimization model for signal timing (Han, Liu, Gayah, Friesz, & Yao, 2016). The authors of the study have considered fuel consumption as a criterion for optimizing signal timings. The authors use traffic microsimulation to test if the algorithm works or not. In another study, the authors develop an optimization model that incorporates multimodal signal priority, coordination, and actuation (He, Head, & Ding, 2014). The authors outline the conflicting issues between actuated-coordination and signal priority requests and develop a mixed integer linear program.

It should be mentioned here that, wireless charging for EVs is still at the early stages of its development. Using currently available technology, the low power of the WCU combined with the relatively short times for charging at intersections would result in very little energy transfer to EVs that use the system. However, it is currently a topic of major research, and it is expected that faster charging technologies (such as Level 3/DC fast charging) will emerge, which will make dynamic charging a feasible alternative for EVs.

3 | DEVELOPMENT OF THE FRAMEWORK

In this section, we describe the WCUM framework development in detail. This framework has four major components, as mentioned in Section 1. In this section, we follow the flowchart in Figure 1 to explain the development. At first, we specify the assumptions behind the framework. Then, we define two optimization problems in two subsections. The optimization problems have different objective functions and constraints. We have used simulation to formulate these functions for the framework. Therefore, we discuss the development of the calibrated simulation model. After that, we describe the process of using the simulation results to formulate the objective functions.

3.1 | Assumptions

The framework development consists of several assumptions, which need to be mentioned before discussing the development of the framework. The assumptions are listed below:

- All signalized intersections are controlled by fully actuated traffic signals.
- All left turn phases are permitted along with the through movement. There are no exclusive left-turn phases at any signal.
- Signal timing parameters will be optimized at an intersection level rather than at the network level. Therefore, signal coordination and associated parameters, such as offset, are not considered in this framework.
- The relationship between the location of WCU and EV routes is not modeled in this framework.

3.2 | Optimization problem formulation

The most important part of the WCUM framework is the two-step optimization problem. At first, we will identify decision variables for the optimization problems. After that, the optimization problems are formulated.

3.2.1 | Variable selection

The analysis starts with the idea that signalized intersections in urban areas are the most suitable locations to place the WCUs on urban arterials. The focus of this study is to maximize the utility of WCUs through EV charging (including both stopped charging and charging in transit over WCUs) at signalized intersections. For fully actuated traffic signal control, there are many parameters that control the traffic operation. In this study, we have chosen minimum green duration (min-green time), maximum green duration (max-green time), and unit extension duration (gap time) as the decision variables (Roess, Prassas, & McShane, 2011). We use signal phase to describe the time interval allocated to one or more simultaneous vehicular traffic movements. For a certain green phase, the min-green time defines the minimum allowable duration of the phase. The max-green time defines the maximum allowable duration up to which a green phase can be extended. The gap time defines the unit

duration which a green phase will be extended for each call from the traffic sensor (e.g., loop detector, camera).

According to National Electrical Manufacturers Association (NEMA) phasing scheme (Roess et al., 2011), the four major through phases are phases 2, 4, 6, and 8 for a standard four-legged intersection. Phases 2 and 6 move together and correspond to the through movement in one direction, and phases 4 and 8 are the conflicting phases corresponding to the through movement in the other direction. In this analysis, the maximum green time of phases 2 and 6 is max-green 1 ($g_{\max 1}$), and the maximum green time of phases 4 and 8 is max-green 2 ($g_{\max 2}$). Similarly, the minimum green time of phases 2 and 6 is min-green 1 ($g_{\min 1}$), and the minimum green time of phases 4 and 8 is min-green 2 ($g_{\min 2}$). The effect of the variables on the utility and control delay is not well defined in the literature. The variations of control delay and utility for each lane depend on the traffic flow patterns and the presence of EVs on that route. The utility of WCUs is dependent on the stopped charging and charging in transit. If a through lane corresponds to phases 2 and 6, then increasing $g_{\max 2}$ (max-green for phases 4 and 8) can increase the utility and control delay of that lane. The reason is that the red phase interval for that approach can increase with the increase of $g_{\max 2}$. Increased red phase intervals means more stopped time for EVs, so more stopped charging is provided. However, more stopped time also means more control delay. On the other hand, increasing $g_{\max 1}$ (max-green for phases 2 and 6) can increase the charging in transit (as more vehicles will cross the WCUs), decrease the stopped charging, and decrease the control delay of that lane. Apart from the minimum and maximum green time, gap time is another parameter that impacts utility and control delay. If a through lane corresponds to phases 2 and 6, then increasing g_t (gap time) can increase the charging in transit (as more vehicles will cross the WCUs), decrease the stopped charging, and decrease the control delay of that lane. However, the gap time of the conflicting phase also increases, which can increase the stopped charging and increase the delay. The gap time is considered equal for approaches in both directions. Besides the traffic signal timing parameters, the number of WCUs has a high impact on the utility value. More WCUs placed back to back will cover a higher proportion of the queue at the intersection, so it has the opportunity to serve more EVs during the stopped time at the intersection. Therefore, we develop both lane- and intersection-specific utility and control delay functions so that we can accurately capture the variations for each lane and intersection separately.

3.2.2 | Intersection-level optimization problem

The optimization strategy for WCU placement consists of two steps. First, we formulate a multiobjective optimization problem for each intersection, where the decision variables are the traffic signal controller parameters. For actuated signals, we have chosen five parameters that affect WCU utility and control delay: the min-green time and max-green time of the phases corresponding to the two through movements (i.e., $g_{\min 1}$, $g_{\min 2}$, $g_{\max 1}$, $g_{\max 2}$), and the gap time (g_t). WCUs are installed along the full length of the approaching lanes of the corresponding intersections. The objective functions are the total utility from all the WCUs and the control delay at the respective intersections. The two objectives are maximization of total intersection utility and minimization of total control delay.

$$\text{Maximize} \quad \sum_{j \in J_i} u_{i,j}(g_{ti}, g_{\min 1i}, g_{\min 2i}, g_{\max 1i}, g_{\max 2i})$$

$$\text{Minimize} \quad \sum_{j \in J_i} CD_{i,j}(g_{ti}, g_{\min 1i}, g_{\min 2i}, g_{\max 1i}, g_{\max 2i})$$

Subject to,

$$CD_{i,j}(g_{ti}, g_{\min 1i}, g_{\min 2i}, g_{\max 1i}, g_{\max 2i}) \le h_{i,j}, \quad \forall i \in I, \forall j \in J_i \tag{1}$$

$$g_{\min\_lower} \le g_{\min 1i}, g_{\min 2i} \le g_{\min\_upper}, \quad \forall i \in I \tag{2}$$

$$g_{\max\_lower} \le g_{\max 1i}, g_{\max 2i} \le g_{\max\_upper}, \quad \forall i \in I \tag{3}$$

$$g_{t\_lower} \le g_{ti} \le g_{t\_upper}, \quad \forall i \in I \tag{4}$$

$$g_{\min 1i}, g_{\min 2i}, g_{\max 1i}, g_{\max 2i} \text{ are integers} \tag{5}$$

where,

I = Set of all signalized intersections

i = Signalized intersection i

J_i = Set of all lanes approaching signalized intersection i

j = Any lane j approaching signalized intersection i

$u_{i,j}$ = WCU Utility function at lane j of intersection i (Wh)

$g_{\min 1i}$ = Minimum green signal time of phases 2 and 6 at intersection i (sec)

$g_{\min 2i}$ = Minimum green signal time of phases 4 and 8 at intersection i (sec)

$g_{\max 1i}$ = Maximum green signal time of phases 2 and 6 at intersection i (sec)

$g_{\max 2i}$ = Maximum green signal time of phases 4 and 8 at intersection i (sec)

$g_{\min\_lower}$ = Acceptable lower value of $g_{\min 1i}$ or $g_{\min 2i}$(sec)

$g_{\min\_upper}$ = Acceptable upper value of $g_{\min 1i}$ or $g_{\min 2i}$(sec)

$g_{\max\_lower}$ = Acceptable lower value of $g_{\max 1i}$ or $g_{\max 2i}$ (sec)

$g_{\max\_upper}$ = Acceptable upper value of $g_{\max 1i}$ or $g_{\max 2i}$(sec)

g_{ti} = Gap time at intersection i (sec)

g_{t_upper} = Acceptable upper value of gap time (sec)

g_{t_lower} = Acceptable lower value of gap time (sec)

$h_{i,j}$ = Control delay limit corresponding to target LOS of lane j at intersection i (sec/veh)

$CD_{i,j}$ = Control delay at lane j of intersection i (sec/veh)

The constraints of the first step of the optimization formulation are range of $g_{\min 1i}$ and $g_{\min 2i}$, range of $g_{\max 1i}$ and $g_{\max 2i}$, range of g_{ti}, and LOS (Highway Capacity Manual, 2010). The purpose of the first step of the optimization is to ensure that increasing the utility of the WCU at any intersection does not degrade the overall operational performance of the intersection. In such a case, the non-EV users will suffer excessive delay, which is not desirable.

The total WCU utility of the intersection is the sum of utility from each lane ($u_{i,j}$) approaching the intersection. Similarly, the total control delay of the intersection is the sum of control delay at each lane ($CD_{i,j}$). In this step, they are both functions of $g_{\min 1i}$, $g_{\min 2i}$, $g_{\max 1i}$, $g_{\max 2i}$, and g_{ti}. There is no limit on the length of WCUs, so WCU is installed across the full length of all the lanes approaching the intersection. There are five constraints of the formulation. The solution to the optimization problem must obey all these constraints. For clarification, the constraints are described below in sequence:

- The control delay of all lanes in each lane group should be less than the threshold value for the target LOS limit. For example, if the target LOS is *C*, then the limiting value of control delay is 35 s/veh (Highway Capacity Manual, 2010) (Equation 1).
- The minimum green signal times of all phases at all the intersections are constrained by an upper and a lower value (Equation 2).
- The maximum green signal times of all phases at all the intersections are constrained by an upper and a lower value (Equation 3).
- The gap time at all the intersections are constrained by an upper and a lower value (Equation 4).
- The min-green times and max-green times are integer constrained (Equation 5).

Scalarization is applied to obtain a single solution. The weighted sum method is used to transform this problem into multiple single objective optimization problems. A weight factor (f_i) is used to calculate the weight of the objective functions in the unified objective function. Different f_i values will yield different solutions, but we will choose only one solution to carry forward to the next step. We sum the utility and control delay for all the lanes at the intersection. Since we will form a minimization problem, we need to invert the total utility value, so that a minimization problem will result in a maximized utility value. Then, we apply feature scaling or unity-based normalization to bring the inverted utility and control delay values between zero and one. Both values should be brought to the same scale; otherwise, the weight of one value will be more than the other in the optimization. After that, we formulate the single objective function with the normalized values. Equation (6) describes the relationship between the unified objective function and the utility, control delay, and the weight factor. The "*ubn*" notation indicates unity-based normalization:

$$z_i = 100 \times (f_i \times ubn((\sum_{j \in J_i} u_{i,j})^{-1}) + (1 - f_i) \times ubn(\sum_{j \in J_i} CD_{i,j})) \quad (6)$$

$$z_i(g_{ti}, g_{\max 1i}, g_{\max 2i}) = k_i \times {g_{ti}}^2 + l_i \times {g_{\max 1i}}^2 + m_i \times {g_{\max 2i}}^2 + n_i \times g_{ti} \times g_{\max 1i} + o_i \times g_{\max 1i} \times g_{\max 2i} + p_i \times g_{\max 2i} \times g_t + q_i \times g_{ti} + r_i \times g_{\max 1i} + s_i \times g_{\max 2i} + t_i \quad (7)$$

where,

$z_i = z_i(g_{ti}, g_{\max 1i}, g_{\max 2i})$ = Objective function value

f_i = Weight factor of intersection i

$k_i, l_i, m_i, \ldots, t_i$ = Coefficients of the second order fitting equation for intersection i

After converting simulation outputs to objective function values, we need to model the relationship between this objective function and the input variables. We assume that the objective function has no variation with $g_{\min 1i}$ and $g_{\min 2i}$. Therefore, we can choose a generic quadratic polynomial of three variables to model a single objective function that combines the utility and control delay functions. The generic quadratic polynomial is shown in Equation (7), which is used to represent the relationship between the single objective function and the input variables ($g_{\max 1i}$, $g_{\max 2i}$, g_{ti}). There are 10 coefficients (k_i-t_i) in this equation, and we need to identify the values of these coefficients for each intersection. We have two data series of 27 data points ($27 = 3^3$ = number of combinations for three independent variables with three values each). One of the data series comes from Equation (6) (simulation outputs) and the other comes from Equation (7). We use a generalized reduced gradient solver to identify the coefficients that minimizes the Root Mean Squared Error (RMSE) between the two data series.

3.2.3 | Network-level optimization problem

The second step of the optimization uses the optimized traffic signal controller parameters (i.e., $g_{\min 1i}$, $g_{\min 2i}$, $g_{\max 1i}$, $g_{\max 2i}$, and g_{ti}) from the previous step to formulate a single objective problem at a network level. In this step, the traffic

control parameters act as constants and do not take part in the optimization process. The decision variable in this step is the number of WCUs placed at the different lanes in each intersection. The objective is the maximization of the total utility from all intersections. The purpose of this step is to determine the spread of the WCUs in the network. The constraint of the optimization formulation in this step is the budget. The objective function is the sum of the WCU utility of each lane ($u_{i,j}$). In this step, the decision variables are the number of installed WCU units ($x_{i,j}$) in lane j at intersection i.

$$\text{Maximize} \sum_{i\in I}\sum_{j\in J_i} u_{i,j}(x_{i,j})$$
$$\text{Subject to,} \quad \sum_{i\in I}\sum_{j\in J_i} x_{i,j}d \le w \tag{8}$$

$$0 \le x_{i,j} \le \frac{l_{i,j}}{y}, \quad \forall i \in I, \forall j \in J_i \tag{9}$$

$$x_{i,j} \text{ is integer} \tag{10}$$

where,

I = Set of all signalized intersection

i = Signalized intersection i

J_i = Set of all lanes approaching intersection i

j = Any lane j approaching signalized intersection i

$u_{i,j}$ = WCU Utility function at lane j of intersection i (Wh)

$x_{i,j}$ = Number of WCU units installed at lane j of intersection i

d = Price of WCU per unit ($/unit)

y = Length of unit WCU (m)

w = Budget ($)

$l_{i,j}$ = Length of lane j of intersection i (m)

There are three constraints of the formulation. The solution to the optimization problem must obey all these constraints. For clarification, the constraints are described below in sequence:

- The total cost of the installation should be less than or equal to the budget (Equation 8).
- The number of WCU units for each lane must be greater than or equal to zero, and less than or equal to the length of the lane divided by unit WCU length (Equation 9).
- The number of WCU units for each lane is integer constrained (Equation 10).

For this step, we follow a similar pattern to the previous step. At first, we use the solutions from the previous step to determine the relationship between the number of WCUs and the utility. When the number of WCU is zero, the utility will always be zero. Apart from that, we evaluate utility values for three data points. Therefore, for each lane, we will have four data points from simulation. A third-order polynomial can accurately capture the relationship for all lanes. Therefore, we calculate the coefficients of the third-order polynomial that passes through all the data points. Equation (11) represents the relationship between number of WCU units and utility for a specific lane:

$$u_{i,j}(x_{i,j}) = a_{i,j} \times {x_{i,j}}^3 + b_{i,j} \times {x_{i,j}}^2 + c_{i,j} \times x_{i,j} + d_{i,j} \tag{11}$$

where,

$a_{i,j}, b_{i,j}, c_{i,j}, d_{i,j}$ = Coefficients of the third-order fitting equation for lane j at intersection i

3.3 | Network calibration and dynamic traffic assignment

In this section, we describe the traffic microsimulation component of the framework. For developing the framework, we have used Simulation of Urban Mobility (SUMO) (Behrisch, Bieker, Erdmann, & Krajzewicz, 2011) as the traffic microsimulation platform of choice, as we can simulate EV and WCU in a calibrated network. SUMO is open source and allows seamless integration to platforms like OpenStreetMap (Haklay & Weber, 2008) and Python.

To create a calibrated traffic simulation model, we need network configuration data (i.e., number of nodes and links, node positions, and link lengths) for the study area, along with OD traffic flow and travel time data. We can collect the Annual Average Daily Traffic (AADT) data and average link speed data from the state DOT's Web site. To convert the AADT of a road segment (link) into a design hourly volume, we need the k-factor (k) and the directional split (d). The k-factor is defined as the factor which converts a daily volume to an hourly volume. The d-factor determines the percentage split of volume in each direction. From previous studies that have collected real-world data across the Sioux Falls area, we can determine the k-factor and directional split. Using these factors, we can convert AADT to Directional Design Hourly Volume (DDHV) using Equation (12):

$$DDHV = AADT \times k \times d \tag{12}$$

The DDHV for each link in SUMO is the ground truth for the DTA model. We have chosen a simulation based DTA model called the Gawron model (Gawron, 1998) for this framework. This model computes the stochastic dynamic user equilibrium for a network using an iterative process. The steps are given below:

- Each vehicle has a finite set of routes and a probability distribution of route choice. In each iteration, a random route

is chosen from the set of routes based on the probability distribution.

- Initially there are no routes in the set. With each iteration, a new route is added to the set based on shortest path calculations, unless the route is already part of the set.
- In each iteration, the travel time and the probability distribution of route choice are updated for each vehicle after routing and microsimulation is performed.
- The model is considered to be converged when the maximum relative standard deviation in travel times between consecutive iterations is below a certain threshold.

$$t_{v,new}(i) = \begin{Bmatrix} t_s, & if\ i = r \\ \beta t_g(i) + (1-\beta)t_v(i), & otherwise \end{Bmatrix} \quad (13)$$

where,

$t_{v,new}(i)$ = Travel time of route i in the current iteration (sec)
$t_v(i)$ = Travel time of route i in the previous iteration (sec)
t_s = Travel time from simulation (sec)
$t_g(i)$ = Sum of time dependent link travel times for route i (sec)
β = Smoothing parameter

Let us consider the routing for one vehicle, v. The set of chosen routes for vehicle v is P_v and the probability distribution is p_v. The sum of the route choice probabilities is always 1. In each iteration, the Gawron model uses SUMO to simulate the network and update the travel times and the probability distributions of route choice for each vehicle. For vehicle v, let us assume that the current selected route is r. The update rule for travel time of all routes in set P_v is given in Equation (13). For route r, the travel time is updated directly from simulation, since the vehicle actually took this route in the previous simulation. For all other routes, the travel time is updated based on the sum of the time-dependent link travel times and the travel time of that route in the previous iteration.

$$p_{v,new}(r) = \frac{p_v(r)[p_v(r) + p_v(s)]e^{\frac{\alpha\delta_{rs}}{1-\delta_{rs}^2}}}{p_v(r)e^{\frac{\alpha\delta_{rs}}{1-\delta_{rs}^2}} + p_v(s)} \quad (14)$$

where,

$p_{v,new}(r)$ = New probability of choosing route r
$p_v(r)$ = Prior probability of choosing route r
$p_v(s)$ = Prior probability of choosing route s
α = Model parameter
δ_{rs} = Relative travel time difference between routes r and s $= \frac{t_v(s)-t_v(r)}{t_v(s)+t_v(r)}$

The new probability of route choice is updated based on the comparison with the travel time of a known route from set P_v. Let us assume that r is the route used in the last iteration and s is another known route in the set P_v. Equation (14) gives the new probability of choosing route r. Equation (15) gives the new probability of choosing a known route. The sum of the prior and new probabilities should be equal.

$$p_{v,new}(s) = p_v(r) + p_v(s) - p_{v,new}(r) \quad (15)$$

where,

$p_{v,new}(s)$ = New probability of choosing route s
$p_{v,new}(r)$ = New probability of choosing route r
$p_v(s)$ = Prior probability of choosing route s
$p_v(r)$ = Prior probability of choosing route r

The method requires the use of a routing algorithm. We have used the well-known Dijkstra's algorithm (Yin & Wang, 2010) in this framework. Significant research has already been conducted in the field of calibration of traffic simulation model (Dowling, Skabardonis, Halkias, McHale, & Zammit, 2004; Hollander & Liu, 2008). We have used a trial and error method to adjust the OD matrix values to match the link DDHV and average travel times with the data from the real world.

3.3.1 | DTA model convergence

Achieving the stochastic dynamic user equilibrium through convergence of an iterative process is a major challenge for any DTA model. The ideal method for testing the convergence of a DTA model is an equilibrium gap function (such as duality gap), which measures the gap between the travel times (or traffic flows) of current iteration and the equilibrium travel times (or traffic flows). However, the equilibrium travel times (or flows) for a large network are not always known, which creates a problem for using gap functions for checking convergence. Therefore, a proxy indicator can be used to measure the change in link travel times in successive iterations to assess if the algorithm has reached a stable solution (Taale & Pel, 2015). In this case, the assumption is that if the link travel times reach a stable value and do not change significantly due to perturbations (i.e., a change in traffic conditions from the previous iteration), such as a congestion buildup, in the following iterations, it can be assumed that the algorithm has reached user equilibrium. In this study, we have used maximum relative standard deviation as the proxy indicator. The condition to terminate the iterations is described using Equation (16).

$$\epsilon(x) = 100\% \times \max_{l \in links} \frac{\sqrt{\frac{\sum_{i=x-d}^{x}\left(tt_l^i - \frac{\sum_{j=x-d}^{x} tt_l^j}{d+1}\right)^2}{d}}}{\frac{\sum_{j=x-d}^{x} tt_l^j}{d+1}} < \epsilon_{th}, \quad d < x \quad (16)$$

where,

$links$ = Set of all links in the network

l = Any link l in the network

x = Current Iteration number

tt_l^i / tt_l^j = Travel time of link l for the ith/jth iteration (s)

$\varepsilon(x)$ = Maximum relative standard deviation for the xth iteration

ε_{th} = Threshold value for maximum relative standard error

d = Number of prior iterations considered for calculation

When the value of ε is below ε_{th}, it is considered that the algorithm has converged and reached a stable solution. The Gawron model ensures that a stable solution can be achieved for any simulation scenario. A stable solution in this case is a stable probability distribution. After a stable solution is reached, a stochastic fluctuation in travel times may result in the variation of δ_{rs}. However, the exponential term $e^{\frac{\alpha\delta_{rs}}{1-\delta_{rs}^2}}$ in Equation (14) ensures that the change in probability distribution due to the change in δ_{rs} is minimal. The parameter α can be used to increase or decrease the sensitivity of the model to stochastic fluctuations in travel times. Figure 2 shows the variation in probability distribution of route choice with respect to the value of α. Decreasing the value of α can increase the stability of the probability function with stochastic variations of δ_{rs} around 0.

Moreover, Gawron has performed a stability analysis of the model, which results in a theoretical limit on the value of α (Gawron, 1998). In the stability analysis performed by Gawron, the effect of a small perturbation on the probability distribution of route choice is examined. The theoretical limit on the value of α is given in Equation (17).

$$\alpha < \frac{\sum_{i=1}^{n} C_i}{\Delta t} \min_{t\in[t_0,t_1]} \frac{\sum_{j=1}^{n} T_j(t)}{d(t)} \tag{17}$$

where,

C_i = Capacity of route i (veh/hr)

$T_j(t)$ = Travel time of route j at time t (sec)

Δt = Congestion period (sec)

$d(t)$ = Total demand at time t (veh/hr)

n = Number of routes in the simulation

t_0 = Start time of congestion (sec)

t_1 = End time of congestion (sec)

From Equation (17), it can be observed that, if the capacities are higher than the demand and the time of congested periods is negligible compared to the overall travel time, the limit on value α is more flexible. However, if the demand matches

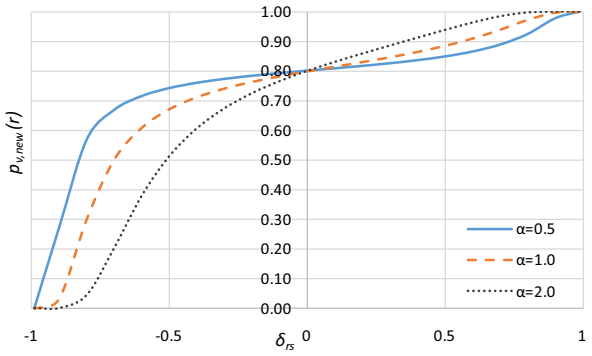

FIGURE 2 Variation of $p_{v,new}(r)$ with δ_{rs} for a simple case with two alternative routes (r and s), where $p_v(r) = 0.8$, $p_v(s) = 0.2$, $\alpha = 0.5$, 1.0, 2.0

capacity and the travel times are similar to congested periods, then the limit on the value of α is very stringent. Therefore, if the users face convergence issues with their test cases, they have two options. They can choose to lower the value of α, which will inherently increase the stability of the probability functions of route choice. The users can also change the value of ε_{th} to achieve fast convergence.

A higher value of α is desired for better performance from the model. However, lowering the value of α increases the stability of the algorithm. Therefore, an optimum value of α can be determined for each case study. If $\alpha = 0$, then the algorithm does not change the route choice probabilities. Equation (17) places an upper limit on the value of α. There is a small range of α in which we can search for the optimal α value, and this range varies between 0 and an upper limit derived from Equation (17). In the simplest setting, a binary search algorithm can be used to determine the optimal value of α. Since the range is bounded from above and below, one can select a value α, verify the convergence, and decrease or increase α to the middle between the upper and lower bound of the updated range based on the convergence estimation. This iteration can be repeated several times gradually updating the current lower and upper bounds of the search range until a proper value of α is found. However, in general, one of the recent trends is to accelerate parameter fitting in simulation using machine-learning approaches. Given sufficient computational resources, one can create a library of simulations, where each simulation is a data point in a feature space. A feature space should include various descriptions and properties of the simulation (i.e., number of nodes/links, link capacities, traffic conditions, etc.). Then, for each of these data points, a label that contains optimized parameters is obtained through actual execution of the simulation. This creates a labeled data set on which a machine learning method can be applied to predict the initial values of the parameters per new test point (a new simulation for which parameters are required). For example, one can use generative neural networks to obtain the acceptable value of α. Such methods are popular in broad

simulation, such as transportation logistics (Wojtusiak, Warden, & Herzog, 2012) and computer architecture design (Hamerly, Perelman, Lau, Calder, & Sherwood, 2006). We can obtain the optimal α value using Equation (17), but it is beyond the scope of this research. In this study, we have obtained the α value from previous case studies and achieved convergence satisfying Equation (16).

3.3.2 | Developing traffic simulation scenarios

Some approximations are made to simplify computations in order to reduce the runtime of the framework. Instead of performing simulation for all possible combinations of min-green times, max-green times, and gap times, we select a low, mid, and high value for each variable, which limits the number of simulation runs within a fixed limit. Using the results from the limited simulation runs, we model the relationship between the variables and the output functions. We assume that the different traffic scenarios at the signalized intersections are accurately represented in the simulation model. Moreover, it is assumed that the utility function and control delay function can be combined into a quadratic polynomial curve-fitting (with exact fitting) equations. Each lane at each intersection will have a different characteristic and finding the accurate relationship of utility and control delay for each lane is a nontrivial task. For simplicity, a quadratic polynomial curve-fitting equation is used.

The calibrated simulation model acts as the base model for this step. The user will assume an EV penetration level when creating the SUMO model files. The traffic simulation cases are created from combinations of low-mid-high values of all the variables ($x_{i,j}$, $g_{\min 1 i}$, $g_{\min 2 i}$, $g_{\max 1 i}$, $g_{\max 2 i}$, and g_{ti}). A high number of cases is generated using this technique. It is difficult to run such high number of simulations using one processor. Therefore, we have developed the framework to run the simulation cases in a Linux-based cluster computer. The WCUM framework is developed using the Palmetto Cluster, which is the primary high-performance computing resource of Clemson University. Palmetto is comprised of 2,021 compute nodes totaling 23,072 CPU cores (Palmetto Cluster user's guide, 2018). The framework pools the requested resources and submits simulation jobs simultaneously. Parallelization is achieved through GNU Parallel (Tange, 2011).

3.4 | Utility calculation

SUMO has a built-in EV energy model and EV charging model (Kurczveil, López, & Schnieder, 2013). The model calculates the energy consumed/charged between the previous timestep and the current timestep for each EV in the simulation. The change in EV energy can be obtained by subtracting the energy loss from the energy gain. Four types of energy gain components are considered, which are: kinetic, potential, rotational, and frictional components. The different resistance components such as acceleration, brake, air drag, and road surface are responsible for the loss of energy. The charging model is based on the relative position of the WCU and the EV at each timestep. Based on the proximity of WCU and EV, the EV battery receives energy from the WCU. The factors that affect the charging are alignment of the coils of EV and WCU, and the time spent by the EV over the WCU. There are two components of charging for an EV, they are stopped charging and charging in transit. Stopped charging refers to the charging of EV at an intersection during the red time interval. It can also be described as opportunistic charging. When an EV approaches the intersection during the green time interval, it gets charged as it passes over the charging coils; this charging is known as charging in transit.

$$u = \sum_{v \in V} \sum_{k=0}^{end\,step} \left(E_{chrg\_stopped,v}(k) + E_{chrg\_transit,v}(k)\right) \quad (18)$$

where,

V = Set of all electric vehicles

v = An electric vehicle v in the network

u = Total utility from a WCU (Wh)

k = Simulation timestep (sec)

$E_{chrg\_stopped,v}(k)$ = Stopped charging of EV v at timestep k (Wh)

$E_{chrg\_transit,v}(k)$ = Charging in transit of EV v at timestep k (Wh)

For each simulation step, the model calculates the energy gain/loss for each EV. An output file is generated from simulation that contains the values of the stopped charging and charging in transit for each EV at each timestep. The output file is used for utility calculation in this framework. Both the EV energy model and EV charging model require input of certain vehicle parameters and charging infrastructure parameters, which can be found in Figure 1.

Equation (18) represents the formula to calculate the utility from one traffic simulation scenario. Here, the utility, u, is the total charging of all the EVs in the network by a WCU. All the charging information from the simulation is generated in an output file. The data from the output file can be parsed and Equation (18) can be used to get the utility value.

3.5 | Control delay calculation

There are many techniques to calculate control delay of an intersection lane group (Highway Capacity Manual, 2010; Ghosh-Dastidar & Adeli, 2006). Among these techniques, the queue-count technique is chosen for the control delay calculation.

The queue-count technique is developed for calculating control delay using traffic data collected from the field. For a specific lane group, the data required from the field is the total vehicle count, stopped vehicles count, vehicles in queue count, approach speed, and cycle length. The stop delay can be calculated from field data. The acceleration and deceleration delay cannot be measured easily; every vehicle that passes through the intersection needs to be tracked individually to measure these delays. The queue-count technique is an established method to provide reasonable approximation of control delay. However, this can only be achieved by applying appropriate adjustment factors (Powell, 1998; Quiroga & Bullock, 1999). In this study, the technique is applied to a simulation environment, where the data collection from the field is mimicked in the simulation. Detectors are used in simulation to collect the input data for the technique. The technique is illustrated using Equations (19)–(23).

$$\text{Time-in-queue per vehicle, } d_{vq} = I_s \frac{V_q}{V_{tot}} \tag{19}$$

$$\text{Fraction of stopped vehicles, } FVS = \frac{V_{stop}}{V_{tot}} \tag{20}$$

$$\text{Number of stopped vehicles/lane/cycle, } V_{qplpc} = \frac{V_{stop}}{N_c \times N} \tag{21}$$

$$\text{Acceleration deceleration correction delay, } d_{ad} = FVS \times CF \tag{22}$$

$$\text{Control delay, } d = d_{vq} + d_{ad} \tag{23}$$

where,

V_{tot} = Total number of vehicles
V_q = Total number of vehicles in queue
V_{stop} = Number of stopped vehicles
N_c = Number of cycles surveyed
S = Approach speed (m/s)
N = Number of Lanes
I_s = Time interval of aggregation (sec)
CF = Acceleration-deceleration correction factor. Values collected from the Highway Capacity Manual (2010) using S and V_{qplpc}

The control delay is calculated to determine LOS for each lane (Highway Capacity Manual, 2010). LOS C is described as the stable flow (acceptable control delay) regime, while LOS D is described as regime approaching unstable flow. The intuitive choice for target LOS criteria should be C, but target LOS is kept as a user input to the model, since it can vary for different situations.

3.6 | Optimization solver selection

The objective functions are nonlinear, and some decision variables are integer constrained, so a global MINLP solver is required for this framework. For MINLP problems, several popular algorithms exist such as branch and bound, branch and cut, genetic algorithm, and ant colony optimization. Many solvers have been developed using these methods. Some of the popular global solvers for MINLP problems are AlphaECP (Lastusilta, Bussieck, & Westerlund, 2009), ANTIGONE (Misener & Floudas, 2014), BARON (Sahinidis, 1996), Bonmin (Bonami & Lee, 2007), Couenne (Belotti, 2009), DICOPT (Grossman et al., 2002), Knitro (Byrd, Nocedal, & Waltz, 2006), LINDOGlobal (Lin & Schrage, 2009), SBB (Bussieck & Drud, 2001), Scip (Achterberg, 2009), Cbc (Forrest & Lougee-Heimer, 2005), and Gurobi (Gu, Rothberg, & Bixby, 2012). To choose the best solver for this framework, a comparative performance evaluation is performed using a case study. The comparison is performed using the NEOS server (Dolan, Fourer, Moré, & Munson, 2002). It is an open access server where users can submit optimization jobs for large-scale problems. However, this framework does not use the NEOS server directly. The server is just a tool which the user can choose to use to find the best solver for the user defined problem. However, the user is required to provide the solver code to the two solver components for our framework.

4 | CASE STUDY

The evaluation of the WCUM framework has been conducted with a case study. The Sioux Falls network (Chakirov, 2016) is chosen as the case study network. The network data, OD traffic flow data, and travel time data for the Sioux Falls network have been made available for public use (Transportation Networks for Research Core Team, 2016). However, this data set does not represent the current traffic conditions. Therefore, we need to collect recent data that represents the current traffic conditions in this area.

The method has been described previously in Section 3.3. We collect the AADT data and the travel time data for the city of Sioux Falls from the South Dakota Department of Transportation (SDDOT) Web site (Turner & Koeneman, 2018). At first, we cross-match the links between this data set and the existing data set to identify the AADT and speed of the links in our case study network. Then, we convert the AADT values to DDHV values using appropriate k-factor and directional split through Equation (12). Based on previous studies for Sioux Falls network, the k-factor value is chosen

as 0.08 and the directional split is chosen as 50% or 0.5 for the whole network. The values are obtained from a major bridge investment study conducted by SDDOT in 2016 (Felsburg Holt & Ullevig & Benesch, 2016).

For this network, the link volumes and speeds are known, but the OD matrix is still unknown. To use the Gawron model for DTA, we need to determine the OD matrix for this network. The OD matrix is initialized using the OD matrix of the Sioux Falls network from the transportation networks repository (Transportation Networks for Research Core Team, 2016). At first, we perform the calibration of the model using the AADT and the speed data. For one specific traffic signal setting, we use the Gawron model to iterate and converge to a user equilibrium. The details of the iterative process can be found in Section 3.3. The values of the Gawron model parameters are obtained from previous studies (Behrisch, Krajzewicz, Wagner, & Wang, 2008) and they have worked well for this case study. The values are, $\alpha = 0.5$, $\beta = 0.9$, $d = 4$, $\varepsilon_{th} = 0.1\%$.

The routes generated by the final iteration of the Gawron model are considered as the final route. However, this assignment does not match the link volumes from the AADT data. Therefore, we continue to adjust the OD matrix and perform dynamic assignment until the solution is within 5% of the DDHV values for every link in the network. This model is considered as the calibrated model. When we change the signal timing parameters in the network, we perform DTA again, since the assignment will change due to the changing link costs influenced by the signal times. However, calibration is not performed again, so the OD matrix remains unchanged.

Figure 3 shows the Sioux Falls road network with node and link numbers. The progression of link flow changes for 20 links (arbitrarily chosen) can be found in Table 1. Table 1 also contains the progression of average travel time per vehicle. It shows how the algorithm is rerouting the vehicles to reduce the travel time. After iteration 8, the algorithm stops because the maximum relative standard deviation in travel time for iterations 4–8 is below 0.1%. At this point, we have reached user equilibrium and the average travel time of the network is 946.3 seconds. After converging to a solution, the final link flows are compared with the DDHV for each link in Table 1. As it can be observed, the link flows change with each iteration, and after iteration 8, it converges to equilibrium values. From Table 1, it can be seen that these link flows are within 5% of the DDHV values for each link, which confirms that this network is a calibrated network. The DTA model did not face any convergence issues with the parameter values mentioned in this section.

Based on the study by Conti et al. (2016), a specific penetration level of EVs has been assumed, which is 10%. The penetration level specifies the probability of a new vehicle generated to be an EV. In the simulation, 45,964 vehicles are generated in 1 hour. The number of EVs generated is 4,548, which is approximately 10% of the total vehicles generated.

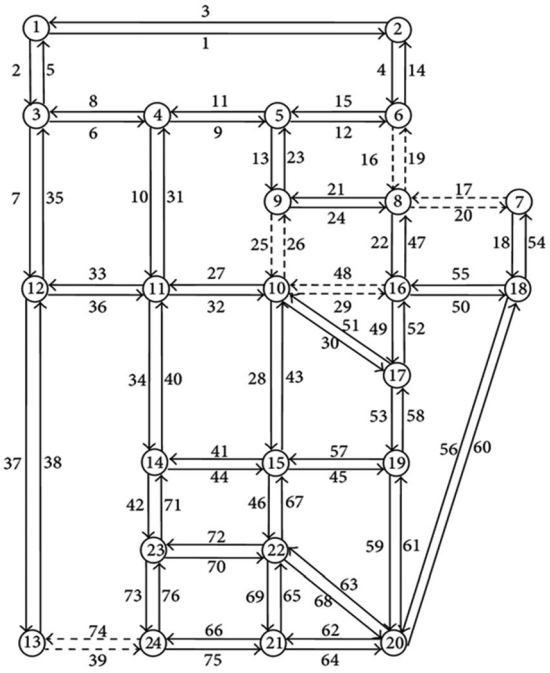

FIGURE 3 Sioux Falls road network with link numbers

The EV generation is uniformly distributed over the network since we do not have the OD data for EV trips. For example, let us assume that 2,000 vehicles are generated from one edge. The 10% EV penetration means that there is a high likelihood that about 200 of those vehicles will be EVs. However, EV penetration rates can vary by location of origin, which will result in a spatial variation of EV flows. The parameters of the EV and WCU model used in this analysis are shown in Table 2. We have used an average efficiency of 85% for the WCU. This is an average based on field tests performed using WCU (Bi et al., 2016). This value includes power loss due to misalignment of charging coils, the air-gap between the coils, the loss at power converters, and the heating loss in the coils. If we increase the efficiency value, it will result in higher utility.

The key characteristics of this road network and a visual representation of the network are shown in Figure 4. There is a text box below the road network diagram that includes the information related to the traffic simulation. The triangles, rectangles, and circles indicate signalized intersections in the network. Triangles indicate no congestion (LOS A-B), rectangles indicate moderate congestion (LOS C), and circles indicate high level of congestion (LOS D-E).

For our analysis, we implemented the framework using SUMO in the Palmetto Cluster at Clemson University. There are 17 signalized intersections and 128 lanes in the network. In the first step, we identify lanes suitable for WCU installation considering length and roadway topology. In the case study, 34 lanes were filtered out in this step.

According to the SCDOT Signal Design Guidelines (2009), based on vehicle approach speed and detector distance from

TABLE 1 DTA and network calibration (average travel time and first 20 link flows in veh/hr)

Average travel time (s/veh)	1050.6	1041.7	970.6	962.3	960.5	951.6	949.4	946.3		
	Flow (veh/hr) in each iteration								Actual flow	Difference between converged
Link no.	1	2	3	4	5	6	7	8	(veh/hr)	flow and actual flow
1	594	642	682	708	827	866	883	908	890	2%
2	1,153	1,210	1,187	1,221	1,210	1,206	1,207	1,211	1,162	4%
3	578	611	613	650	654	659	675	678	696	3%
4	621	616	668	695	815	854	868	889	868	2%
5	1,173	1,239	1,259	1,275	1,383	1,415	1,420	1,442	1,419	2%
6	1,024	807	774	756	745	736	730	727	717	1%
7	1,380	1,633	1,561	1,566	1,548	1,532	1,528	1,526	1,503	2%
8	1,000	1,701	1,704	1,738	1,866	1,908	1,938	1,978	1,968	1%
9	1,348	1,132	1,068	1,051	962	954	944	934	983	5%
10	430	466	610	639	703	721	731	742	728	2%
11	1,359	1,429	1,477	1,470	1,526	1,536	1,535	1,546	1,605	4%
12	830	601	546	509	497	486	474	464	487	5%
13	1,068	1,201	1,312	1,368	1,407	1,426	1,443	1,451	1,492	3%
14	600	587	596	638	640	644	655	661	673	2%
15	764	952	1,116	1,151	1,326	1,354	1,372	1,392	1,417	2%
16	1,266	910	755	711	703	712	701	705	718	2%
17	1,029	765	762	770	767	765	758	754	726	4%
18	1,155	1,083	1,018	988	978	962	952	944	921	2%
19	1,180	1,232	1,254	1,298	1,361	1,372	1,388	1,409	1,367	3%
20	949	783	728	715	712	708	697	697	673	4%

TABLE 2 EV and WCU properties and corresponding values

Specification	Properties	Value
EV	Air Drag Coefficient	0.3
	Front Surface Area	0.8 m^2
	Internal Moment of Inertia	0.01 kgm^2
	Maximum Battery Capacity	54 KWh
	Propulsion Efficiency	0.9
	Radial Drag Coefficient	0.2
	Recuperation Efficiency	0.9
	Roll Drag Coefficient	0.01
	Vehicle Mass	1700 Kg
	Initial Battery Capacity	27 KWh (50%)
WCU	Length of one WCU	6 m
	Budget Constraint	6 units
	Charging Delay	0s
	Efficiency	85%
	Power Rating of each WCU	7.2 KW

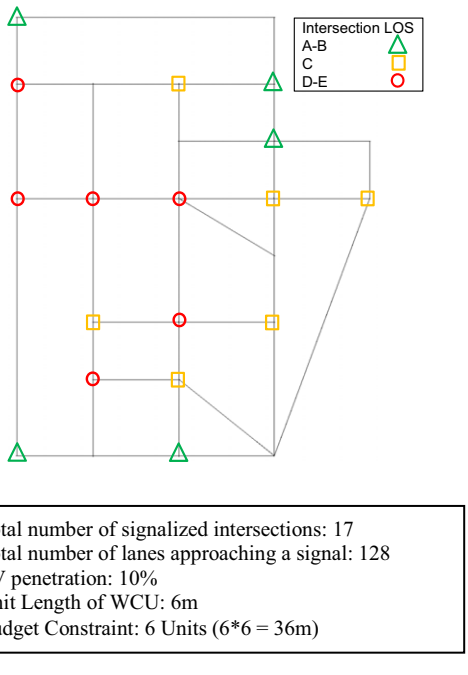

FIGURE 4 Sioux Falls road network in SUMO

stop bars, the allowable minimum green time varies between 8 and 15 seconds for this case study. Using this range, after analyzing initial simulation results from our case study network, we have observed that the variation of g_{min1} and g_{min2} for an intersection has little impact on the lane and intersection specific utilities and control delays. The maximum variation

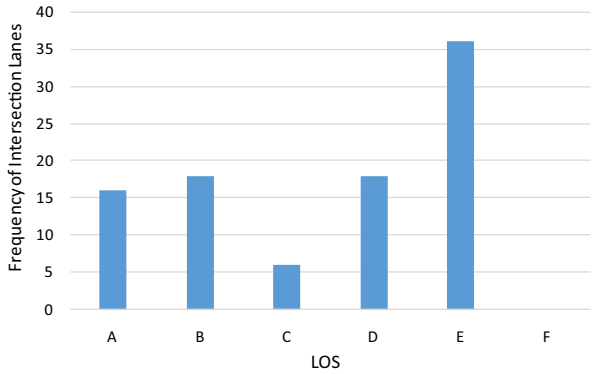

FIGURE 5 Frequency distribution of all intersection lanes by LOS

found from simulation turned out to be insignificant (0.1%). The control delay showed no variation with min-green times. The reason is sufficient traffic demand on all approaches and low range of allowable values. For this case study, minimum green is omitted as a decision variable from the analysis. To do that, we have used 15 seconds as the $g_{\text{min\_lower}}$ and $g_{\text{min\_upper}}$ time, fixing the value of min-green times to 15 seconds.

From Section 3, we know that the user needs to specify some additional inputs for the optimization steps. For this case study, the max-green time range is 20–50 seconds, and the gap time range is 1–3 seconds (SCDOT Signal Design Guidelines, 2009). These are inputs to the framework, so the ranges will vary based on the signal design practices/guidelines and user judgment corresponding to the selected network. The user will determine the appropriate range of values and input the values. After running the simulations, the postprocessing of simulation output data is performed. This step contains the parsing of large XML files to calculate the utility and control delay from each simulation case following the method described in Sections 3.4 and 3.5, respectively.

As mentioned previously, we have 94 lanes approaching traffic signals. In Figure 5, we have drawn the histogram plot of the LOS of all 94 lanes during the simulation. The LOS has been measured based on the control delay. From Figure 5, it is observed that 54 out of the 94 lanes operate in LOS D and E, so the network operates in a congested condition.

5 | ANALYSIS AND FINDINGS FOR CASE STUDY

We present results from the analysis of the WCUM framework for the case study. Later analysis shows the comparison of WCUM framework with two other WCU placement frameworks (i.e., betweenness centrality-based framework and traffic volume-based framework).

5.1 | Optimization solution and solver comparison

After the utility and control delay calculations, it is desired to find the optimal lanes to place the WCUs such that the utility is maximized while intersection operation remains acceptable. At first, we solve the optimization problem at an intersection level, and then we solve the optimization problem at a network level.

5.1.1 | Test of difference between objective function and simulation output

Intersection-level optimization problem includes solving a multiobjective optimization problem for each intersection. There are 17 intersections in this network, so we solve 17 multiobjective optimization problems. For each problem, the two objective functions are as follows: intersection-specific utility-related objective function and control delay function. These two objective functions are converted into a single objective function. The conversion to a single objective function has been previously described in Section 3.2.2. Here, we describe the analysis using a sample intersection, Intersection 6.

Based on the method in Section 3.2.2, we first calculate the coefficients of Equation (7). To validate the coefficients, we conduct a statistical hypothesis test (an F-test followed by a t-test) to determine the difference between the two data series. Before conducting the test, we check the normality of the two data sets. We perform multiple normality tests and find that both data sets can be modeled according to a normal distribution.

We conduct the tests for different weight factors to validate the method. We perform the F-test to check for difference in variances, and the two-sample t-test to check for difference in means between the two data series at a 95% confidence interval ($\alpha = 0.05$). For all tests, the null hypothesis is that the variances (F-test)/means (t-test) are equal. The F-test and t-test results are summarized in Table 3. All the observed p-values are higher than the α (0.05) value; the lowest observed p-value is 0.15 for F-test and 0.69 for t-test. Based on the statistical analysis and RMSE values, it is proved that the difference between the objective function in Equations (6)

TABLE 3 F-test and t-test results for different weights

Factors (f values)	F-test (p value)	t-test (p value)	RMSE
0	0.15	1.00	11.6
0.1	0.24	0.69	8.9
0.3	0.39	0.72	6.1
0.5	0.57	0.81	3.6
0.7	0.52	1.00	11.3
0.9	0.44	0.97	5.2
1	0.29	0.92	5.3

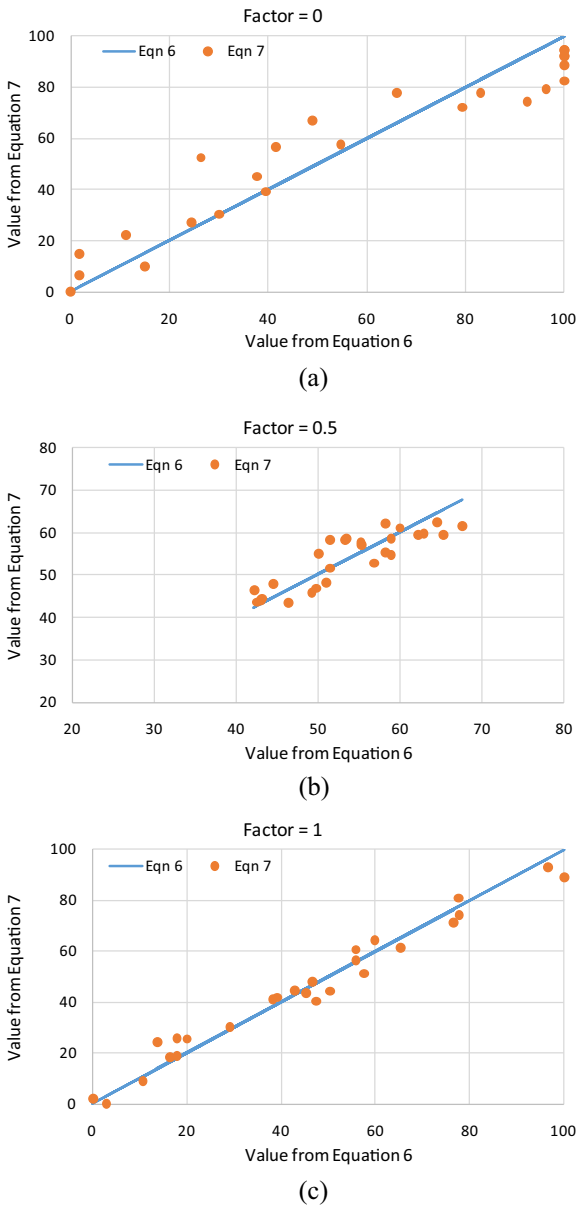

FIGURE 6 Comparison of output from Equation (6) and Equation (7) (intersection 6). (a) Factor = 0. (b) Factor = 0.5. (c) Factor = 1

and (7) is insignificant. Equation (7) is used for calculating the objective function value in the remainder of the analysis. The comparison of Equations (6) and (7) is shown graphically in Figure 6 for three factors (0, 0.5, and 1).

5.1.2 | Solution and comparison: Intersection-level optimization

As mentioned in Section 5.1.1, at first, we calculate the objective function values for each combination of variables from simulation output using Equation (6). Then, we find the coefficients of Equation (7) for each intersection. Then, we solve the intersection-level optimization problem we discussed in Section 3.2.2. To identify the best optimization solver for this problem, we solve the optimization problem using the different solvers mentioned in Section 3.6. The objective function is nonlinear, and two of the three decision variables (i.e., $g_{\max 1}$ and $g_{\max 2}$) are integer constrained. This results in a MINLP problem for each intersection. We also want to achieve a global solution to the optimization problem. Here, we have compared 12 solvers for solving MINLP problems. The solutions have been compared based on two criteria, computation time and solution quality. The results of the optimization are shown in Table 4, and the comparison of solution quality (minimized objective value) and computation time for different solvers is shown in Figure 7.

Couenne and ANTIGONE are the two best solvers for this optimization. They both achieve the best solution (43.498) in 2 ms. Couenne consistently performs well for other intersections also. Couenne uses a branch and bound algorithm to solve mixed integer nonlinear problems. Couenne performs well in obtaining global optimum solution for both convex and nonconvex problems. Therefore, we choose Couenne as the solver for intersection-level optimization.

The purpose of scalarization here is to convert the multi-objective optimization to multiple single objective optimization problems. In this study, for each intersection, we have varied the values from 0 to 1 with 0.1 increments. This has resulted in 11 solutions for each intersection. The criteria for choosing f are based on the control-delay solution values for each factor. An example is presented with intersection 6. The variation of the solution with different factors is shown in Table 5. From Table 5, we can observe that, the minimum control delay that can be achieved is 20 s/veh, corresponding to LOS C. When the f value is increased from 0 to 0.5, the control delay is 32 s/veh, which is still within the range of LOS C. If f is set to 0.6, the solution exceeds 35 s/veh (threshold for LOS C). Therefore, the selected f value for intersection 6 is 0.5. A similar analysis is performed for all other intersections.

We use the Couenne solver and the corresponding weight factors to solve the optimization problems for all 17 intersections. The results for each intersection are shown in Table 6. In the first step of the optimization, for all 17 intersections, we have performed optimization considering two scenarios, (a) maximizing utility and minimizing control delay, and (b) minimizing only control delay. The resulting utility and control delays, for both scenarios, are shown in Table 6. As it can be observed, the control delay for all intersections are equal or lower when utility is not considered in the optimization compared to the control delay when both utility and control delay are considered in the optimization. This shows that, when the utility is maximized while minimizing the control delay, then control delay increases because the two objectives are conflicting. There are some intersections that are heavily congested, where the control delay cannot be reduced beyond a

TABLE 4 Results from different solvers (optimization for intersection 6)

Solvers	Algorithm	g_t (s)	g_{max1} (s)	g_{max2} (s)
AlphaECP	Extended cutting plane (ECP)	2	50	20
ANTIGONE	Deterministic Solver	3	50	20
BARON	Branch and Reduce	1	50	35
Bonmin	Hybrid outer-approximation based branch-and-cut	3	50	50
Couenne	Branch-and-bound	2	50	35
DICOPT	Extended outer-approximation	1	20	47
Knitro	Interior-point/Active Set	2	20	20
LINDOGlobal	Branch-and-cut	3	50	20
SBB	Branch-and-bound	3	20	20
Scip	Branch-and-cut-and-price	3	20	20
Cbc	COIN-OR Branch and Cut	2	50	50
Gurobi	Generalized Reduced Gradient	1	35	35

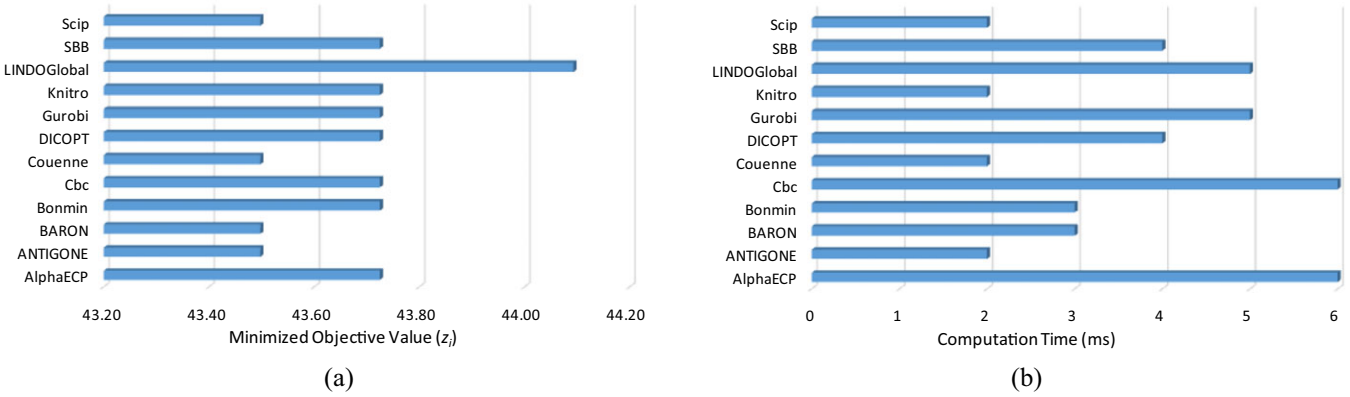

FIGURE 7 Comparison of different solvers (intersection 6). (a) Solution quality. (b) Computation time

TABLE 5 Selection of f value for intersection 6

Factors (f values)	Utility	Control delay
0	1,216	20
0.1	1,216	20
0.2	1,216	20
0.3	1,216	20
0.4	1,432	26
0.5	1,627	32
0.6	1,742	41
0.7	1,998	64
0.8	3,877	73
0.9	3,877	73
1	3,877	73

certain point. Intersections 2 and 5 operate in LOS E and intersection 12 operates in LOS D regardless of the strategy. For the other intersections, the control delay is increased because utility is part of the objective function. However, a comparison of the two control delays (column 6 and column 8 in Table 6) shows that an increase in control delay, due to considering the utility maximization in addition to the control delay minimization, is such that the LOS (shown inside parentheses of column 6 and 8) is not degraded. This is achieved by choosing the solution (f value) from a set of solutions for which the utility is the maximum and the control delay is within the range of the target LOS (i.e., LOS considering only minimizing average control delay and without considering the total utility maximization objective). For example, for intersection 6, the selected value of f is 0.5. For this f value, the control delay is increased from 20 s/veh to 32 s/veh. However, the control delay is within the range of the target LOS C (20–35 s/veh). The utility is increased by 385 KWh in this case. From Table 5, we have already observed that, if f value is increased more than 0.5, the optimization produces a solution for which utility is higher than 1,627 KWh but the LOS is degraded to D from LOS C.

Although we have minimized the delay in this step, not all intersections have a delay corresponding to LOS C. Therefore, we will not include the lanes from the intersection that have LOS more than C in the network-level optimization. The network-level optimization should select lanes that have a LOS C or better than LOS C. The assumption here is

TABLE 6 Intersection-level optimization solution using Couenne

Column 1	Column 2	Column 3	Column 4	Column 5	Column 6	Column 7	Column 8
				Maximizing utility and minimizing control delay		Minimizing only control delay	
Intersections	g_t, sec	g_{max1}, sec	g_{max2}, sec	Total utility, KWh	Average control delay, s/veh (LOS)	Total utility, KWh	Average control delay, s/veh (LOS)
1	2	50	20	625	9 (A)	617	7 (A)
2	3	50	20	3,099	64 (E)	3,099	64 (E)
3	1	50	35	561	10 (A)	537	7 (A)
4	3	50	50	1,356	31 (C)	1,086	21 (C)
5	2	50	35	3,520	61 (E)	3,520	61 (E)
6	1	20	47	1,627	32 (C)	1,242	21 (C)
7	2	20	20	1,474	29 (C)	1,320	25 (C)
8	3	50	20	521	5 (A)	521	5 (A)
9	3	20	20	721	20 (B)	583	11 (B)
10	3	20	20	1,213	31 (C)	977	21 (C)
11	2	50	50	724	20 (B)	648	13 (B)
12	1	35	35	2,166	47 (D)	2,166	47 (D)
13	3	35	35	1,557	34 (C)	1,508	32 (C)
14	1.8	20	50	2,031	34 (C)	1,456	21 (C)
15	1.7	20	50	785	20 (B)	674	11 (B)
16	3	50	20	282	6 (A)	276	5 (A)
17	1.4	43	20	2,120	32 (C)	1,807	21 (C)

that the operation of those intersections will improve in the future.

An assumption in this step is that all the lanes of an intersection have WCU installed throughout the lane. In this step of the optimization, there is no budget constraint, so WCU can be installed in the full length of the lane. We consider the maximum potential length of the lanes for charging. This is a valid assumption for the first step of the optimization, since one of the objectives of the signal timing parameter optimization is maximizing utility values at each intersection. In the second step of the optimization, the budget is included as a constraint, which will limit the number of WCUs that can be installed in each lane.

5.1.3 | Solution and comparison: Network-level optimization

In the second step of the optimization, there is only one maximization objective, and the decision variables are the number of WCU units at each lane. As we have already ascertained the max-green times and the gap times, these values will be constant for this step of the optimization. In the case study, there are 94 variables (for 94 lanes) in this step.

The method described in Section 3.2.3 is used in this section. We determine the coefficients of Equation (11) for all intersections. All the variables for this problem are integer constrained, and the total utility is sum of all the utility functions. The budget constraint assumed for this section is six WCU units, and the optimization solution will tell us where to place these six units. Then, we solve the network-level optimization problem using different solvers in the NEOS server. The solvers that we evaluate in this section are the same as the ones we used in the previous step. The optimization results from the solvers are shown in Table 7, and the comparison of different solvers is shown in Figure 8.

From the analysis, it is observed that the maximum utility that can be achieved is 71.55 KWh. For this step, Couenne is the best solver in terms of solution quality and computation time. Four lanes (lanes 29, 37, 38, and 82) from three intersections (intersections 6, 7, and 15) have been selected for WCU installation. The budget constraint allowed a maximum of six units of installation, so the distribution of units is 1, 1, 3, and 1, respectively, for lanes 29, 37, 38, and 82. The total utility achieved (total energy charged in KWh) from this experiment is 71.55 KWh. This corresponds to about 120 miles of additional range supplied to EVs. The control delay of lanes 29, 37, 38, and 82 are 32, 29, 29, and 20 s/veh, respectively. The graphical representation of the installation solution can be seen in Figure 9. The square filled boxes indicate the selected intersections and the number inside the box indicates the lane number at that intersection which has been selected.

TABLE 7 Results from different solvers (network-level optimization)

Solvers	Lane 20 (Int. 4)	Lane 29 (Int. 6)	Lane 37 (Int. 7)	Lane 38 (Int. 7)	Lane 70 (Int. 13)	Lane 82 (Int. 15)	Maximized utility value (KWh)
AlphaECP		1	1	3		1	71.55
ANTIGONE		1	1	3	1		71.45
BARON		2	1	3			71.20
Bonmin		1	1	3		1	71.55
Couenne		1	1	3		1	71.55
DICOPT				6			63.36
Knitro		2	1	3			71.20
LINDOGlobal		2	1	3			71.20
SBB		1	1	3		1	71.55
Scip	1			3	1	1	69.59
Cbc		1	1	3		1	71.55
Gurobi		1	1	3		1	71.55

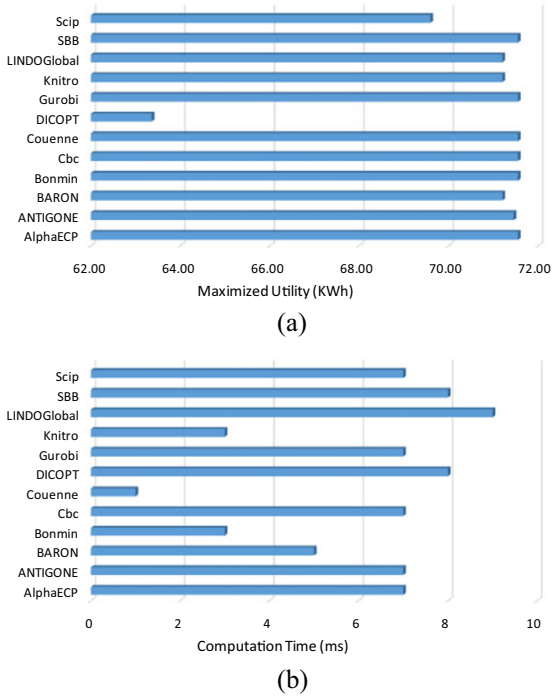

FIGURE 8 Comparison of different solvers. (a) Solution quality. (b) Computation time

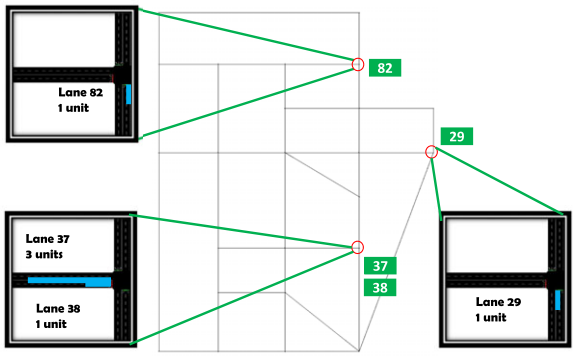

FIGURE 9 Optimization output

5.2 | Analysis of the framework solution

We need to analyze the output generated from the optimization step. The optimization framework is able to achieve 71.55 KWh of charging from four different lanes. On average, the WCUs provide 188 Wh of energy to an EV. Typically, 188 Wh of energy equals 0.5 miles of additional range for each charged EV in the simulation. From the 71.55 KWh, about 56.45 KWh of charging occurs while EVs are stopped at the intersections. The rest of the charging occurs while in transit. The maximum charging achieved by a single EV is 1.12 KWh, which is equivalent to approximately 2 miles of additional range. The total number of generated EVs is 4,548 but the total number of charged EVs is 223. Therefore, only 5% of the generated EVs are charged during the simulation.

The utility values of the lanes have a complex relationship with the EV traffic flow and the control delay at the intersection. From the results, it can be observed that stopped charging is closely related with control delay, and charge-in-transit is closely related with number of EVs charged. Lane 38 is the best lane in terms of utility, since the highest number of WCUs (3) is installed in this lane. Lane 38 charges EVs at the rate of 354 Wh/EV. Among the other three lanes, lane 29 has the next highest amount of total charging (11.66 KWh) but also has high EV flow and high control delay, so the average charging is 124 Wh/EV. Lanes 37 and 82 have similar characteristics in terms of average charging. The results are shown in Table 8.

TABLE 8 Analysis of the optimization results

Lanes	Total charging (KWh)	Stopped charging (KWh)	Charge-in-transit (KWh)	EVs charged	Average charging (Wh/EV)	Average control delay (s/veh)
29	11.66	8.75	2.91	104	124	32
37	10.91	8.73	2.18	78	140	29
38	38.28	30.62	7.66	98	354	29
82	10.70	8.35	2.35	80	134	20

5.3 | Alternative frameworks

In this section, we investigate two simple models for WCU installation, the betweenness centrality-based WCU allocation model (Brandes, 2001) and the traffic volume-based allocation model.

The betweenness centrality is a widely used concept in network science that measures node significance based on the node's presence in the agent paths. In this study, we have already performed the DTA and achieved user equilibrium. Therefore, we use the equilibrium routes of vehicles to perform the centrality calculations. In a directed graph with multiple nodes, each node can be part of multiple equilibrium paths. However, we need to rank the links instead of the nodes. We use the betweenness centrality for ranking the links by assuming that a link is a node in the case study network. A link is connected to another link if they share an intersection (node) between them. Equation (24) gives the betweenness centrality of a link r.

$$g(r) = \sum_{p \neq r \neq q} \frac{\sigma_{pq}(r)}{\sigma_{pq}} \tag{24}$$

where,

σ_{pq} = Total shortest path count from edge p to edge q

$\sigma_{pq}(r)$ = Total shortest path count from edge p to edge q that pass through edge r

Based on betweenness centrality, the link with the highest betweenness centrality value is chosen. The WCU of maximum allowable length based on budget (6 units or 36 m in this study) is placed at different lanes in the selected link to identify the lane that yields the maximum utility. Multiple simulation cases are performed and in each simulation case, the WCU is placed in a different lane on the selected link. The simulations are performed using SUMO. The utility achieved from betweenness centrality-based WCU allocation model is 63.36 KWh.

The framework is also compared with another deployment paradigm called traffic volume-based allocation model. The lane with the highest traffic volume is found by placing detectors on all lanes in the simulation and extracting the traffic flow for each lane. This paradigm has very low computational requirements. It achieves utility of 41.59 KWh.

TABLE 9 Comparison of utility from different models

Strategy	Utility (Wh)	Relative difference with respect to WCUM framework
WCUM Framework Model	71.55	-
Betweenness Centrality based WCU Allocation Model	63.36	−12%
Traffic Volume based WCU Allocation Model	41.59	−42%

The model comparison is represented in Table 9. The WCUM framework achieves higher utility from the same number of WCUs. However, there are many other factors associated with the real-world deployment of WCUs. To prove the superiority of a deployment scheme, a cost–benefit analysis should be performed. The focus of this study is developing a framework for WCU deployment. Therefore, we have not performed an economic analysis to determine the feasibility of the deployment plan in this study. This framework can be used in future studies to develop methods that consider the economic aspect of the WCU deployment process.

6 | CONTRIBUTIONS OF THIS RESEARCH

In this study, a novel framework (WCUM) is developed, which uses a traffic micro simulation model of a network of any area and identifies (a) the placement and sizing of WCUs and (b) the traffic signal timing parameters (minimum and maximum green times, and gap times), which maximize the utility of the deployment (total amount of wireless charging in KWh) within a given budget and minimize the traffic signal control delay at each intersection. The novelty in the approach lies in the development of a framework that finds the optimal locations for WCU installation in urban areas using the concept of opportunistic and in-motion charging at traffic signals. To the best of our knowledge, this is the first study that incorporates fully actuated traffic signals, DTA model, and traffic microsimulation model in the

analysis of finding the optimal locations to install the WCUs in the network. The framework has been developed using SUMO traffic simulator, Gawron DTA model, and Couenne solver, but they can be replaced by any other traffic microsimulator, DTA model, and MINLP solver. Moreover, the two-step optimization formulation reduces the computational complexity of the framework. Due to the intersection-level optimization, the complexity of the network-level optimization problem decreases. Instead of doing simulation-based optimization, we create a framework that reduces the computational burden by doing the simulations in a preprocessing step and developing higher-order polynomials for the optimization step. We demonstrate that the developed framework is able to identify the optimal locations to place the WCUs while obtaining higher utility compared to betweenness centrality and traffic volume-based WCU application methods, maintaining operationally acceptable intersection LOS and reducing the computation time. This is the first study that simultaneously maximizes the utility of WCU deployment while minimizing the traffic signal control delay within a given budget. The traffic microsimulation-based approach to optimal installation is also a new concept for CWD application. Previous work has focused on EV energy management and routing strategies based on location of EV charging facilities. However, the concepts of our focus were not present in previous work. The framework also has an advantage of scalability; it can be used for large-scale networks with thousands of signalized intersections.

7 | CONCLUSION AND FUTURE WORKS

The WCUM framework can be considered a first step for developing WCU deployment frameworks in the future. One major limitation of this framework is the economic aspect, which can be incorporated in the framework in future. Some assumptions have been made while developing this framework, which have been mentioned in Section 3.1. In future work, we can investigate a unified optimization model that optimizes the signal timing parameters and the location of WCU simultaneously. A network-level optimization problem can be formulated instead of intersection-level optimization problem to optimize the signal timing parameters. Moreover, we can explore complex phasing patterns other than the simple one we have used in the article. The routing of EVs can be incorporated into the optimization model so that more EVs can be charged by the WCUs, thus increasing the utility of the WCU deployment.

This research will provide the building blocks for further work in the field of dynamic wireless charging for EVs. Actuated signals are increasingly replaced with adaptive signal control that varies signal phases and timing parameters based on real-time conditions as detected by roadway sensors, and the number of signals operating in this manner will increase in the future at the same time that WCU technology is maturing and is being implemented. So, this study can be extended to investigate the effects of adaptive signals on CWD at signalized intersections. In this article, it is also assumed that the interaction between the signalized intersections is negligible. However, often coordination exists among the signals on a corridor, which has not been considered here. This factor can be included in future work.

Connected Vehicle Technology can be incorporated in EVs, which will allow the EVs to interact with roadside infrastructure, such as traffic signals and charging stations, for data sharing. A smart real-time charge scheduling method can be developed for EVs, which will consider routing based on location of EV charging stations and WCUs on the road network. In addition, vehicle-to-infrastructure communication with traffic signals can further increase the utility for WCUs for connected EVs. A routing strategy can be developed for WCU that will take the connected EVs to the nearby charging stations for urgent charging needs.

ACKNOWLEDGMENTS

This research is supported by the National Science Foundation under Award #1647361. Any opinions, findings, conclusions, or recommendations expressed in this material are those of the authors and do not necessarily reflect the views of the National Science Foundation.

Clemson University is acknowledged for generous allotment of compute time on Palmetto Cluster.

REFERENCES

Achterberg, T. (2009). SCIP: Solving constraint integer programs. *Mathematical Programming Computation*, *1*(1), 1–41.

Behrisch, M., Bieker, L., Erdmann, J., & Krajzewicz, D. (2011). SUMO–simulation of urban mobility: An overview. In *Proceedings of SIMUL 2011, The Third International Conference on Advances in System Simulation*. ThinkMind.

Behrisch, M., Krajzewicz, D., Wagner, P., & Wang, Y. P. (2008). Comparison of Methods for Increasing the Performance of a DUA Computation. In *DTA2008 International Symposium on Dynamic Traffic Assignment* (No. EPFL-CONF-154989).

Belotti, P. (2009). *Couenne: A user's manual* (Vol. 3). Technical report, Lehigh University.

Bešinović, N., Quaglietta, E., & Goverde, R. M. P. (2017). Microscopic models and network transformations for automated railway traffic planning. *Computer-Aided Civil and Infrastructure Engineering*, *32*(2), 89–106.

Bhavsar, P., He, Y., Chowdhury, M., Fries, R., & Shealy, A. (2014). Energy consumption reduction strategies for plug-in hybrid electric vehicles with connected vehicle technology in urban areas.

Transportation Research Record: Journal of the Transportation Research Board 2424, 29–38.

Bi, Z., Kan, T., Mi, C. C., Zhang, Y., Zhao, Z., & Keoleian, G. A. (2016). A review of wireless power transfer for electric vehicles: Prospects to enhance sustainable mobility. *Applied Energy*, *179*, 413–425.

Bonami, P., & Lee, J. (2007). BONMIN user's manual. *Numerical Mathematics*, *4*, 1–32.

Brandes, U. (2001). A faster algorithm for betweenness centrality. *Journal of Mathematical Sociology*, *25*(2), 163–177.

Bussieck, M. R., & Drud, A. (2001). *SBB: A new solver for mixed integer nonlinear programming*. Retrieved online from http://www.gams.com/presentations/or01/sbb.pdf

Byrd, R. H., Nocedal, J., & Waltz, R. A. (2006). KNITRO: An integrated package for nonlinear optimization. In *Large-scale nonlinear optimization* (pp. 35–59). US: Springer.

Caíno-Lores, S., García, A., García-Carballeira, F., & Carretero, J. (2017). Efficient design assessment in the railway electric infrastructure domain using cloud computing. *Integrated Computer-Aided Engineering*, *24*(1), 57–72.

Chakirov, A. (2016). *Sioux Falls. The Multi-Agent Transport Simulation MATSim*, 385–388. https://doi.org/10.5334/baw.59

Chen, Z., He, F., & Yin, Y. (2016). Optimal deployment of charging lanes for electric vehicles in transportation networks. *Transportation Research Part B: Methodological*, *91*, 344–365.

Cirimele, V., Freschi, F., & Guglielmi, P. (2014). Wireless power transfer structure design for electric vehicle in charge while driving. In *2014 International Conference on Electrical Machines (ICEM)*, IEEE, 2461–2467.

Conti, J., Holtberg, P., Diefenderfer, J., Larose, A., Turnure, J. T., & Westfall, L. (2016). *International energy outlook 2016 with projections to 2040*. Report No. DOE/EIA-0484 (2016). USDOE Energy Information Administration (EIA), Washington, DC: Office of Energy Analysis.

Deflorio, F., Guglielmi, P., Pinna, I., Castello, L., & Marfull, S. (2015). Modeling and analysis of wireless "Charge While Driving" operations for fully electric vehicles. *Transportation Research Procedia*, *5*, 161–174.

Dolan, E. D., Fourer, R., Moré, J. J., & Munson, T. S. (2002). Optimization on the NEOS server. *SIAM News*, *35*(6), 4.

Dowling, R., Skabardonis, A., Halkias, J., McHale, G., & Zammit, G. (2004). Guidelines for calibration of microsimulation models: Framework and applications. *Transportation Research Record: Journal of the Transportation Research Board*, 1876, 1–9.

Egbue, O., & Long, S. (2012). Barriers to widespread adoption of electric vehicles: An analysis of consumer attitudes and perceptions. *Energy Policy*, *48*, 717–729.

Ehrgott, M. (2006). A discussion of scalarization techniques for multiple objective integer programming. *Annals of Operations Research*, *147*(1), 343–360.

Felsburg Holt & Ullevig & Benesch. (2016). *Major bridge investment study*. South Dakota Department of Transportation. FHU Reference No. 14-381. Retrieved from. http://www.sddot.com/transportation/highways/planning/specialstudies/docs/SDDOTMajorBridgeStudy.pdf

Forrest, J., & Lougee-Heimer, R. (2005). CBC user guide. *INFORMS Tutorials in Operations Research*, 257277.

Fuller, M. (2016). Wireless charging in California: Range, recharge, and vehicle electrification. *Transportation Research Part C: Emerging Technologies*, *67*, 343–356.

Gawron, C. (1998). *Simulation based traffic assignment: Computing user equilibria in large street networks* (Doctoral dissertation, Verlag nicht ermittelbar).

Ghosh-Dastidar, S., & Adeli, H. (2006). Neural network-wavelet microsimulation model for delay and queue length estimation at freeway work zones. *Journal of Transportation Engineering*, *132*(4), 331–341.

Gill, J. S., Bhavsar, P., Chowdhury, M., Johnson, J., Taiber, J., & Fries, R. (2014). Infrastructure cost issues related to inductively coupled power transfer for electric vehicles. *Procedia Computer Science*, *32*, 545–552.

Grossmann, I. E., Viswanathan, J., Vecchietti, A., Raman, R., & Kalvelagen, E. (2002). GAMS/DICOPT: A discrete continuous optimization package. GAMS Corporation Inc.

Gu, Z., Rothberg, E., & Bixby, R. (2012). *Gurobi Optimizer reference manual*, Version 5.0. Gurobi Optimization Inc., Houston, USA.

Haklay, M., & Weber, P. (2008). Openstreetmap: User-generated street maps. *IEEE Pervasive Computing*, *7*(4), 12–18.

Hamerly, G., Perelman, E., Lau, J., Calder, B., & Sherwood, T. (2006). Using machine learning to guide architecture simulation. *Journal of Machine Learning Research*, *7*(Feb), 343–378.

Han, K., Liu, H., Gayah, V. V., Friesz, T. L., & Yao, T. (2016). A robust optimization approach for dynamic traffic signal control with emission considerations. *Transportation Research Part C: Emerging Technologies*, *70*, 3–26.

He, F., Yin, Y., & Lawphongpanich, S. (2014). Network equilibrium models with battery electric vehicles. *Transportation Research Part B: Methodological*, *67*, 306–319.

He, Q., Head, K. L., & Ding, J. (2014). Multi-modal traffic signal control with priority, signal actuation and coordination. *Transportation Research Part C: Emerging Technologies*, *46*, 65–82.

He, Y., Chowdhury, M., Pisu, P., & Ma, Y. (2012). An energy optimization strategy for power-split drivetrain plug-in hybrid electric vehicles. *Transportation Research Part C: Emerging Technologies*, *22*, 29–41.

Highway Capacity Manual. (2010). HCM2010. *Transportation Research Board*. Washington, DC: National Research Council.

Hollander, Y., & Liu, R. (2008). The principles of calibrating traffic microsimulation models. *Transportation*, *35*(3), 347–362.

Jang, Y. J., Ko, Y. D., & Jeong, S. (2012). Optimal design of the wireless charging electric vehicle. In *2012 IEEE International Electric Vehicle Conference (IEVC)* IEEE, 1–5.

Johnson, J., Chowdhury, M., He, Y., & Taiber, J. (2013). Utilizing real-time information transferring potentials to vehicles to improve the fast-charging process in electric vehicles. *Transportation Research Part C: Emerging Technologies*, *26*, 352–366.

Johnson, J., Chowdhury, M. A., He, Y., & Taiber, J. (2012). Facilitating the battery charging process in electric vehicles through connected

vehicle and infrastructure. *Proceedings of the 91st Transportation Research Board Annual Meeting*, Washington, D.C.

Ko, Y. D., & Jang, Y. J. (2013). The optimal system design of the online electric vehicle utilizing wireless power transmission technology. *IEEE Transactions on Intelligent Transportation Systems*, *14*(3), 1255–1265.

Kurczveil, T., López, P. Á., & Schnieder, E. (2013). Implementation of an energy model and a charging infrastructure in SUMO. In *Simulation of Urban MObility User Conference*. Berlin, Heidelberg: Springer, 33–43.

Lastusilta, T., Bussieck, M. R., & Westerlund, T. (2009). An experimental study of the GAMS/AlphaECP MINLP solver. *Industrial & Engineering Chemistry Research*, *48*(15), 7337–7345.

Li, S., Huang, Y., & Mason, S. J. (2016). A multi-period optimization model for the deployment of public electric vehicle charging stations on network. *Transportation Research Part C: Emerging Technologies*, *65*, 128–143.

Li, S., & Mi, C. C. (2015). Wireless power transfer for electric vehicle applications. *IEEE Journal of Emerging and Selected Topics in Power Electronics*, *3*(1), 4–17.

Lin, Y., & Schrage, L. (2009). The global solver in the LINDO API. *Optimization Methods & Software*, *24*(4-5), 657–668.

Lukic, S., & Pantic, Z. (2013). Cutting the cord: Static and dynamic inductive wireless charging of electric vehicles. *IEEE Electrification Magazine*, *1*(1), 57–64.

Marler, R. T., & Arora, J. S. (2010). The weighted sum method for multi-objective optimization: New insights. *Structural and Multidisciplinary Optimization*, *41*(6), 853–862.

Misener, R., & Floudas, C. A. (2014). ANTIGONE: Algorithms for continuous/integer global optimization of nonlinear equations. *Journal of Global Optimization*, *59*(2-3), 503–526.

Mohrehkesh, S., & Nadeem, T. (2011). Toward a wireless charging for battery electric vehicles at traffic intersections. In *2011 14th International IEEE Conference on Intelligent Transportation Systems (ITSC)*, IEEE, 113–118.

Palmetto Cluster user's guide. (2018). Retrieved from https://www.palmetto.clemson.edu/palmetto/userguide_palmetto_overview.html

Powell, J. (1998). Field measurement of signalized intersection delay for 1997 update of the highway capacity manual. *Transportation Research Record: Journal of the Transportation Research Board*, 1646, 79–86.

Qiu, C., Chau, K. T., Liu, C., & Chan, C. C. (2013). Overview of wireless power transfer for electric vehicle charging. In *2013 World Electric Vehicle Symposium and Exhibition (EVS27)*, IEEE, 1–9.

Quiroga, C. A., & Bullock, D. (1999). Measuring control delay at signalized intersections. *Journal of Transportation Engineering*, *125*(4), 271–280.

Riemann, R., Wang, D. Z., & Busch, F. (2015). Optimal location of wireless charging facilities for electric vehicles: Flow-capturing location model with stochastic user equilibrium. *Transportation Research Part C: Emerging Technologies*, *58*, 1–12.

Roess, R. P., Prassas, E. S., & McShane, W. R. (2011). *Traffic engineering* (4th ed.). Upper Saddle River, NJ: Pearson. ISBN-13: 978-0-13-613573-9.

Sahinidis, N. V. (1996). BARON: A general purpose global optimization software package. *Journal of Global Optimization*, *8*(2), 201–205.

Sarker, A., Qiu, C., Shen, H., Gil, A., Taiber, J., Chowdhury, M., … Rindos, A. J. (2016). An efficient wireless power transfer system to balance the state of charge of electric vehicles. In *2016 45th International Conference on Parallel Processing (ICPP)*, IEEE, 324–333.

SCDOT Signal Design Guidelines. (2009). Retrieved from http://www.scdot.org/business/pdf/accessMgt/trafficEngineering/2009_Signal_Design_Guidelines.pdf

Taale, H., & Pel, A. (2015). Better convergence for dynamic traffic assignment methods. *Transportation Research Procedia*, *10*, 197–206.

Tange, O. (2011). GNU Parallel-the command-line power tool. *The USENIX Magazine*, *36*(1), 42–47.

Transportation Networks for Research Core Team. (2016). *Transportation networks for research*. Retrieved from https://github.com/bstabler/TransportationNetworks

Turner, S. M., & Koeneman, P. (2018). *Validating the National Performance Management Research Data Set (NPMRDS) for South Dakota* (No. SD2013-08-F). South Dakota Department of Transportation, Office of Research.

Ushijima-Mwesigwa, H., Khan, M. D., Chowdhury, M. A., & Safro, I. (2017). Optimal installation for electric vehicle wireless charging lanes. arXiv preprint arXiv:1704.01022

Vilathgamuwa, D. M., & Sampath, J. P. K. (2015). Wireless power transfer (WPT) for electric vehicles (EVS)—Present and future trends. In *Plug in electric vehicles in smart grids*. Singapore: Springer, 33–60.

Wang, R., Zhou, Z., Ishibuchi, H., Liao, T., & Zhang, T. (2018). Localized weighted sum method for many-objective optimization. *IEEE Transactions on Evolutionary Computation*, *22*(1), 3–18.

Wojtusiak, J., Warden, T., & Herzog, O. (2012). Machine learning in agent-based stochastic simulation: Inferential theory and evaluation in transportation logistics. *Computers & Mathematics with Applications*, *64*(12), 3658–3665.

Yin, C., & Wang, H. (2010). Developed Dijkstra shortest path search algorithm and simulation. In *IEEE 2010 International Conference on Computer Design and Applications*, V1-116–V1-119.

How to cite this article: Khan Z, Khan SM, Chowdhury M, Safro I, Ushijima-Mwesigwa H. Wireless charging utility maximization and intersection control delay minimization framework for electric vehicles. *Comput Aided Civ Inf*. 2019;1–22. https://doi.org/10.1111/mice.12439